Dispersion characteristics of guided waves in functionally graded anisotropic micro/nano-plates based on the modified couple stress theory

Cancan Liu, Jiangong Yu, Wei-Jiang Xu, Xiaoming Zhang, Xianhui Wang

Dispersion characteristics of guided waves in functionally graded anisotropic micro/nano-plates based on the modified couple stress theory

Cancan Liu [a], Jiangong Yu [a,*], Weijiang Xu [b], Xiaoming Zhang [a], Xianhui Wang [a]

[a] *School of Mechanical and Power Engineering, Henan Polytechnic University, Jiaozuo, 454003, PR China*

[b] *Univ. Polytechnique Hauts-de-France, CNRS, Univ. Lille, YNCREA, Centrale Lille, UMR 8520 – IEMN, DOAE, F-59313, Valenciennes, France*

In this paper, the acoustic wave motion characteristics of Lamb and SH waves in functionally graded (FG) anisotropic micro/nano-plates are studied based on the modified couple stress theory. A higher efficient computational approach, the extended Legendre orthogonal polynomial method (LOPM) is utilized to deduce solving process. This polynomial method does not need to solve the FG micro/nano-plates hierarchically, which provides a more realistic analysis model for FG micro/nano-plates and has high computational efficiency. Simultaneously, the solutions based on the global matrix method (GMM) are also deduced to verify the correctness of the polynomial method. Furthermore, the effects of size and material gradient are studied in detail. Numerical results show that the size effect causes wrinkles in Lamb wave dispersion curves, and the material gradient characteristic changes the amplitude and range of wrinkles. For SH waves, the length scale parameter L_x increases the cut-off frequency but does not change the overall trend of the dispersion curve; on the contrary, L_z does not change the cut-off frequency but causes the dispersion curve to show an upward trend.

1. Introduction

Recently, the nanoelectromechanical (NEMS) and micro-electromechanical systems (MEMS) have promoted intensive researches of small-scale structures. The scale effect of mechanical properties is one of the most important issues in the application of micro/nano-structures. Due to this effect, the classical mechanics theory and numerical methods have been greatly challenged in the study of mechanical properties (such as wave motion, vibration, buckling, etc.). The couple stress theory is one of the continuum mechanics theories which can capture the size-dependency of small-scale structures. The indeterminate couple stress theory with uncertain spherical part of couple stress tensor and two additional constants is developed by Mindlin and Tiersten [1]. Subsequently, by extracting the couple stress moment tensor symmetrically, Yang et al. [2] proposed a modified couple stress theory that involves only one material length scale parameter. Chen and Li [3] presented a modified couple stress theory for anisotropic micro-structures with the length scale parameters in three different directions considered. In this theory, the new constitutive relationships are established by setting the couple stress moment tensor to be symmetric. The couple stress curvature tensor is asymmetric, but the couple stress moment tensor is symmetric. The modified couple stress theory for anisotropic micro-structures has

been used to solve the bending, free vibration and buckling of anisotropic layered micro-plates [4] and the buckling of anisotropic piezoelectric cylindrical shells [5]. It pointed out that there is no evidence to limit this theory to the specific crystal shape of the materials in open literatures, but it may be realized in the future and further research.

Micro/nano-plates, micro/nano-shafts and micro/nano-beams of different complexity are the basis for designing the MEMS and NEMS. These micro/nano-structures are often subjected to dynamic working loads as elastic waves, and their dynamic response can be evaluated by analyzing the elastic wave propagation characteristics. Recently, the couple stress theory has been widely used to study the size effect of bending wave [6], Lamb wave [7,8], and Rayleigh waves [9]. In addition, many works have also studied the size effect of elastic wave propagation based on nonlocal theory [10,11], surface effect theory [12,13], nonlocal strain gradient theory [14], and micropolar theory [15].

Functionally graded materials (FGM) are known as the newborn category of composites, and their material properties change continuously from one face to the other. Their main advantage is that high stress concentrations at the layer interfaces can be eliminated [16,17]. Functionally graded (FG) micro/nano-structures (such as micro/nano-films, micro/nano-plates) have also shown great application potential in micro/nano-electromechanical, micro/nano-electronics, physics and
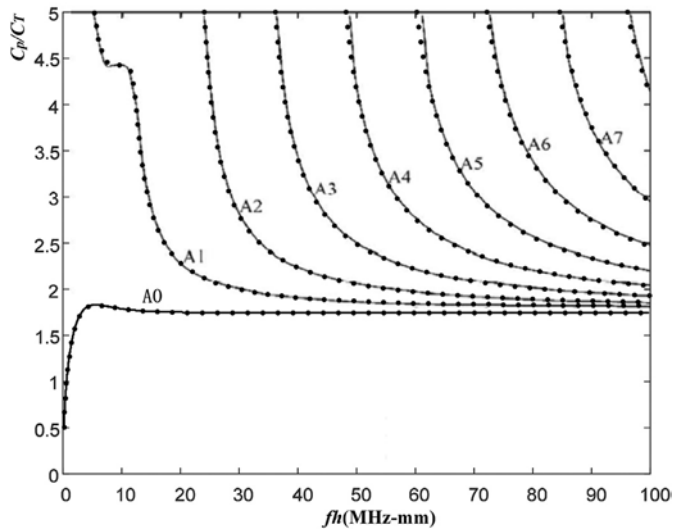

Table 1
Phase velocity of the first-order Lamb wave mode obtained using LOPM.

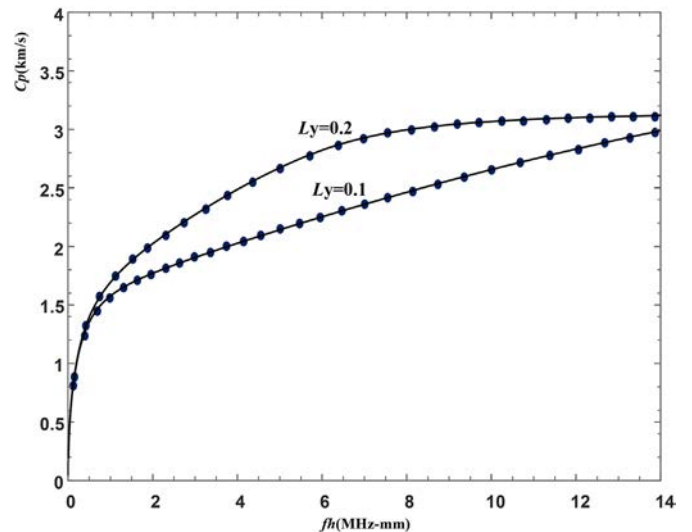| M	$kh = 10$	$kh = 20$	$kh = 30$	$kh = 40$	$kh = 50$	$kh = 60$
9	3.00285	2.86923	2.76619	2.70451	2.66754	2.64858
10	3.00285	2.86906	2.76598	2.70400	2.66338	2.63720
11	3.00284	2.86903	2.76584	2.70394	2.66272	2.63390
12	3.00284	2.86901	2.76579	2.70389	2.66264	2.63321
13	3.00284	2.86899	2.76578	2.70386	2.66262	2.63308

Fig. 1. Dispersion curves in skew-symmetric modes of Lamb waves in a plate of aluminum nitride. Solid lines: the results from Ref. [8]; dot lines: the results obtained using LOPM.

Fig. 2. Dispersion curves of the first Lamb wave modes for an FG anisotropic couple-stressed plate; solid lines: the results obtained using LOPM; dot lines: the results obtained using GMM.

biology fields. In recent years, the size-dependent continuum models for FG structures have been the focuses of many scientific studies. The thermal and mechanical buckling analysis of FG graphene nanoplatelets (GNPs) was studied based on modified strain gradient theory [18]. Sahmani and Safaei [19] investigated the nonlinear free vibrations of bi-directional functionally graded micro/nano-beams. In addition, the wave motion in FG structures has also received sufficient attention. Based on the nonlocal strain gradient theory, the flexural wave propagation analysis for FG micro-beam was studied by Li et al. [20]. Considering the rectangular cross-section, wave propagation analysis for FG nano-beam was investigated via nonlocal elasticity theory [21]. The size-dependent guided wave propagation in porous FG nanoplates was studied with considering nonlocal elasticity theory [22].

Recently, the modified couple stress theory has been used to investigate the new mechanical behaviors of FG structures [23,24]. Beside, as an important group of material, anisotropic micro/nano-structures have attracted many researcher's attention [25]. The wave dispersion in anisotropic doubly-curved shells was studied based on a new nonlocal strain gradient higher order shell theory [26]. **Liu et al. [27] studied the reflection behavior of the elastic waves in orthotropic couple-stressed materials.** Guo et al. [28] studied the size-dependent behavior of FG anisotropic composite plates using the couple stress

theory. For FG anisotropic micro/nano-structures with great application potential, the study of the wave propagation characteristics can provide a theoretical basis for its design and performance prediction. It can be seen from the literature review that the wave propagation in typical micro/nano-structures have been extensively studied. However, there seems a lack of investigation on the Lamb and SH wave propagation characteristics in FG anisotropic micro/nano-plates employing the couple stress theory.

As a series of common methods for solving wave propagation in composite structures, the traditional matrix methods (such as transfer matrix method (TMM) and global matrix method (GMM)) are particularly difficult to solve the wave propagation problem with considering the size effect, anisotropy and FG structure characteristics at the same time. For the first point, the displacement solutions and boundary conditions in the context of the couple stress theory are much more complicated than those in the context of classical elastic theory. For the second point, the Christoffel equation must be solved to determine the wave propagation vectors in the anisotropic micro/nano structure. For the third point, it needs to use the multi-layer model to approximate the FG micro/nano-structure. The above points bring great difficulties to numerical calculations. This motivates the authors to extend the Legendre orthogonal polynomial method (LOPM) to investigate the dispersion relations of Lamb and SH waves in FG micro/nano-plates. Since LOPM does not need to solve the FG structure hierarchically, it has been widely utilized to study guide wave propagation in various FG macro-structures [29–31]. Considering the couple stress effect, Liu et al. [32] developed LOPM to calculate the reflection and transmission coefficients of FG micro-plates immersed in liquid. Different from the previous work, this paper extends the LOPM to study guided wave propagation in micro/nano-structures by introducing the couple stress theory.

Table 2
Material constants of PZT-4 and PZT-5A (C_{ij} in 10^9 N/m^2) [36].

	C11	C22	C33	C44	C55	C66	C12	C13	C23
PZT-4	139.0	139.0	115.0	25.6	25.6	30.6	77.8	74.3	74.3
PZT-5A	99.201	99.201	86.856	21.1	21.1	22.593	7.95	6.10	6.92

Table 3

Material constants of BaTiO$_3$ and Human tibia (ρ in 10^3 kg/m^3 and C_{ij} in 10^9 N/m^2).

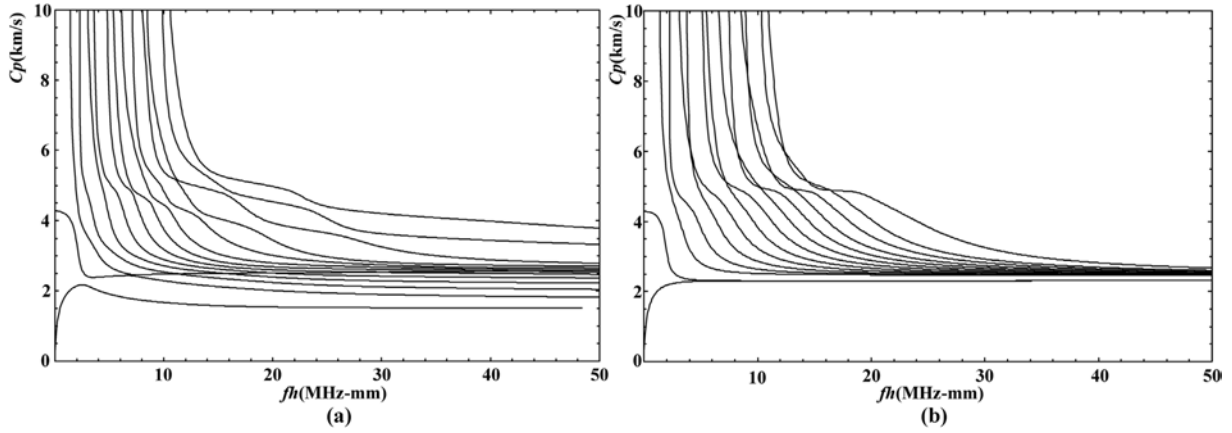|	C11	C22	C33	C44	C55	C66	C12	C13	C23	ρ
BaTiO$_3$	166	166	162	43	43	44.5	77	78	78	5.8
Human tibia	11.6	14.4	22.5	4.91	3.56	2.41	7.95	6.10	6.92	1.8

Fig. 3. The Lamb wave dispersion curves for homogeneous and FG plates without considering the effect of couple stress; (a) FGM plate, (b) homogeneous plate.
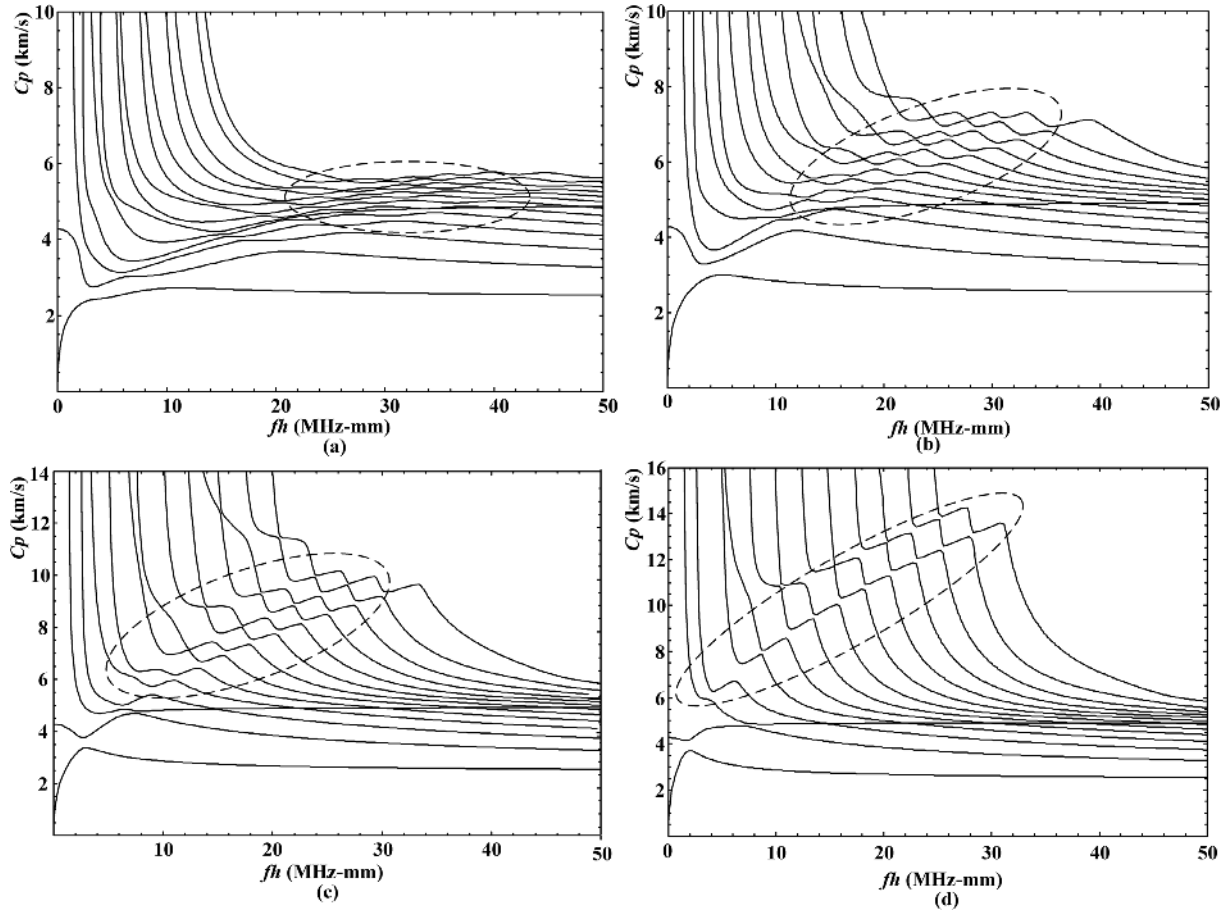

Fig. 4. Dispersion curves of Lamb waves in an FG micro/nano-plate made of BaTiO$_3$ and human tibia with the couple stress. (a): $L_y = 0.1$ (b):$L_y = 0.2$ (c): $L_y = 0.4$ (d): $L_y = 0.8$.
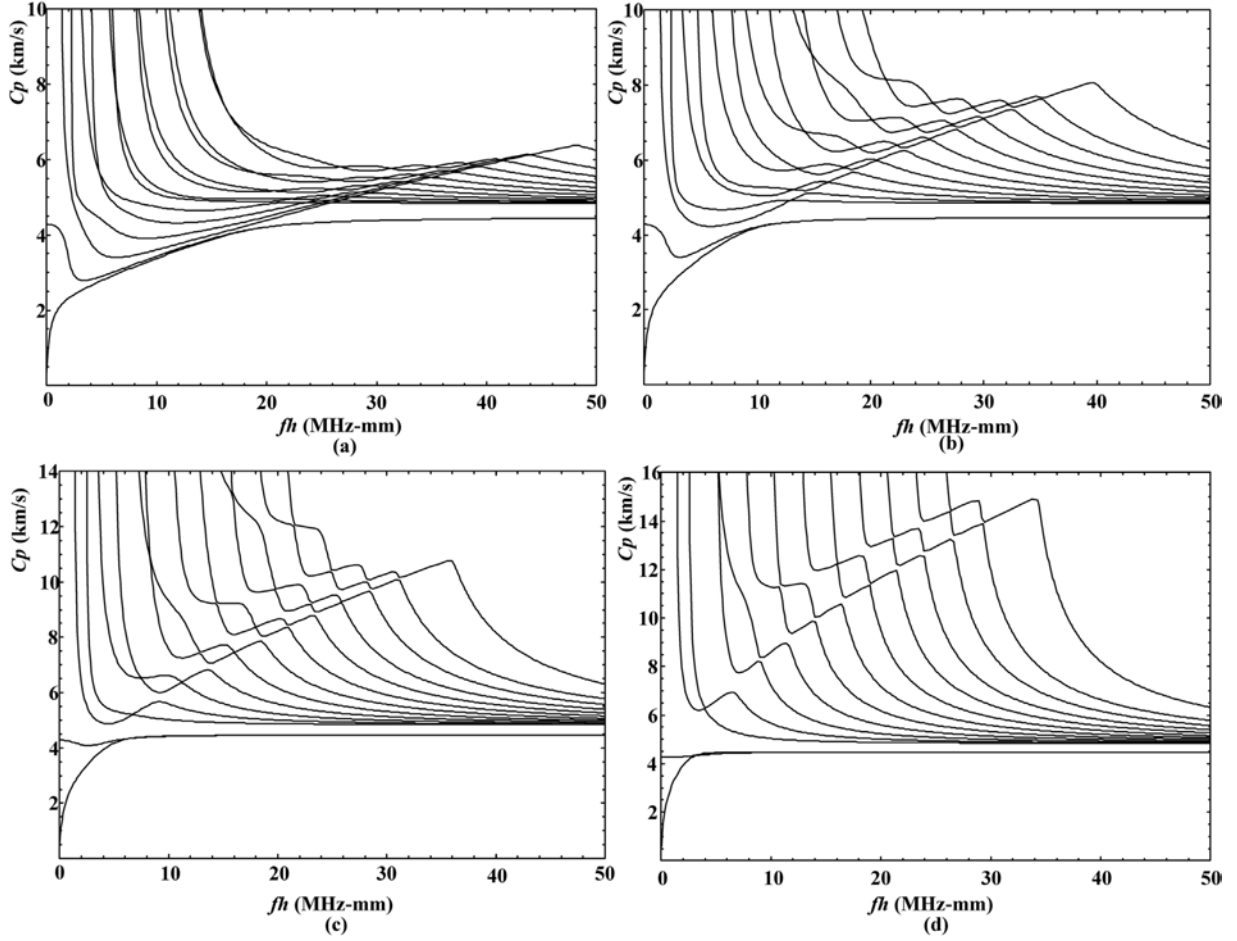
3

Fig. 5. Dispersion curves of Lamb waves in a homogeneous micro/nano-plate made of BaTiO$_3$ and human tibia with the couple stress. (a): $L_y = 0.1$ (b):$L_y = 0.2$ (c): $L_y = 0.4$ (d): $L_y = 0.8$.
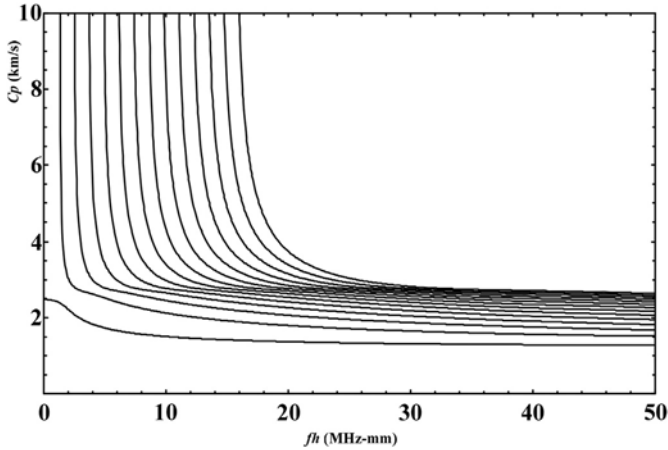

Fig. 6. Dispersion curves of SH waves in an FG plate made of BaTio$_3$and human tibia without considering the effect of couple stress.

2. Problem statement and mathematical formulation

2.1. Basic equations

According to the modified couple stress theory proposed by Chen et al., the constitutive relations and governing equations of the aniso-tropic elastic material are given by Refs. [3,4].

$$\sigma_{li,l}^s + \frac{1}{2}\xi_{ijk}\mu_{lk,lj} = \rho..u_i,$$

$$\sigma_{ij}^s = C_{ijkl}\varepsilon_{kl},$$

$$\varepsilon_{ij} = \frac{1}{2}\left(u_{i,j} + u_{j,i}\right),$$ (1)

$$\mu_{ji} = l_i^2 G_i \omega_{i,j} + l_j^2 G_j \omega_{j,i},$$

$$\omega_i = \frac{1}{2}\xi_{ijk}u_{k,j},$$

where comma indicates partial differentiation, and the double dot (¨) represents the second derivative with respect to time; u_i, ε_{ij} and σ_{ji}^s represent the displacements, strain components and symmetric portions of the stress, respectively; ω_i and μ_{ji} represent the rotation and couple stress vectors; C_{ijkl} and ρ are the material elastic constants and mass density, respectively. G_i ($i = x, y, z$) and l_i ($i = x, y, z$) are the shear elastic constants and length scale parameters in different directions.

An FG plate with thickness h is considered. It is composed of two single materials whose volume content changes in the z direction. Using the Voigt-type model [33], the effective material constant $P(z)$ can be expressed as:

$$P(z) = P_1 V_1(z) + P_2 V_2(z),$$ (2)

The effective material constant $P(z)$ can represent functions of elastic constants and density: $\rho(z)$ and $C_{ijkl}(z)$. P_1 and P_2 are the material constants of the two materials respectively. $V_1(z)$ and $V_2(z)$ represent the

4

volume fraction of two materials respectively, where $V_1(z) + V_2(z) = 1$. Taking the power-law function distribution into consideration, $P(z)$ can be shown as:

$$P(z) = P_2 + (P_1 - P_2)V_1(z), \ V_1(z) = \left(\frac{z}{h}\right)^n, \ 0 \le z \le h, \tag{3}$$

2.2. Formulation of the problem

The position-dependent physical constants can easily incorporate the boundary conditions into the equations of motion. The theoretical bases for how position-dependent physical constants fulfil this role has been detailed in Ref. [34].

By introducing the rectangular window function $\pi(z)$ given by the position-dependent physical constants:

$$\pi(z) = \begin{cases} 1, 0 \le z \le h \\ 0, elsewhere \end{cases} \tag{4}$$

The stress-free and couple stress-free boundary condition ($\sigma_{zz} = \sigma_{zx} = \mu_{zy} = 0$ at $z = 0$ and $z = h$) are automatically incorporated in the constitutive relations of the anisotropic couple stress plate:

$$\sigma_{ij}^s = C_{ijkl}(z)\varepsilon_{kl}\pi(z),$$
$$\mu_{ji} = \left(l_i^2 G_i(z)\omega_{i,j} + l_j^2 G_j(z)\omega_{j,i}\right)\pi(z), \tag{5}$$

For guided waves propagating in a plate along the x direction, the displacement components can be in the following form:

$$u_x = U(z)\exp[i(kx - \omega t)], \tag{6a}$$

$$u_y = V(z)\exp[i(kx - \omega t)], \tag{6b}$$

$$u_z = W(z)\exp[i(kx - \omega t)], \tag{6c}$$

where k is the wave number, and ω is the angular frequency.

For orthotropic materials, substituting Eqs. (5) and (6) into Eq. (1), the governing equations become:

where the superscript ()' indicates the partial derivative for z.

Eq. (7c) is independent of Eqs. (7a) and (7b), and Eq. (7a) is coupled with Eq. (7b). In fact, Eq. (7c) controls SH waves, while Eqs. (7a) and (7b) control Lamb-type waves. The results of Lamb waves are only associated to the length scale parameter l_y. The results of SH wave are associated to the length scale parameters l_x and l_z.

To resolve the equations, the $U(z)$, $V(z)$ and $W(z)$ are expanded to the Legendre orthogonal polynomial series [35]:

$$U(z) = \sum_{m=0}^{\infty} p_m^1 Q_m(z), V(z) = \sum_{m=0}^{\infty} p_m^2 Q_m(z), W(z) = \sum_{m=0}^{\infty} p_m^3 Q_m(z), \tag{8}$$

where p_m^1, p_m^2 and p_m^3 represent the undetermined polynomial coefficients and:

$$Q_m(z) = \sqrt{\frac{2m+1}{h}}P_m\left(\frac{2z-h}{h}\right). \tag{9}$$

where P_m is the Legendre polynomials of order m. The value of m should reach infinity theoretically. In the calculation process, when the influence of high-order polynomial terms can be ignored, the value of m is taken to the cut-off order value M.

Substituting Eqs. (8) and (9) into Eq. (7), and multiplying by $Q_j(z)$ with j running from 0 to M, then integrating over z from 0 to h, give the following equations:

$$A_{11}^{j,m}p_m^1 + A_{12}^{j,m}p_m^2 + A_{13}^{j,m}p_m^3 = -\omega^2 M_m^j p_m^1 \tag{10a}$$

$$A_{21}^{j,m}p_m^1 + A_{22}^{j,m}p_m^2 + A_{23}^{j,m}p_m^3 = -\omega^2 M_m^j p_m^2 \tag{10b}$$

$$A_{31}^{j,m}p_m^1 + A_{32}^{j,m}p_m^2 + A_{33}^{j,m}p_m^3 = -\omega^2 M_m^j p_m^3 \tag{10c}$$

Eq. (10) can be written in a matrix form as:

$$\begin{bmatrix} A_{11}^{j,m} A_{12}^{j,m} A_{13}^{j,m} \\ A_{21}^{j,m} A_{22}^{j,m} A_{23}^{j,m} \\ A_{31}^{j,m} A_{32}^{j,m} A_{33}^{j,m} \end{bmatrix} \begin{bmatrix} p_m^1 \\ p_m^2 \\ p_m^3 \end{bmatrix} = -\omega^2 \begin{bmatrix} M_m^j & 0 & 0 \\ 0 & M_m^j & 0 \\ 0 & 0 & M_m^j \end{bmatrix} \begin{bmatrix} p_m^1 \\ p_m^2 \\ p_m^3 \end{bmatrix} \tag{11}$$

$$\left(-k^2 C_{11}(z)U(z) + \left(1+0.25k^2l_y^2\right)C_{55}'(z)U'(z) + \left(1+0.25k^2l_y^2\right)C_{55}(z)U''(z) - 0.25l_y^2 C_{55}''(z)U''(z) - 0.5l_y^2 C_{55}'(z)U'''(z) - 0.25l_y^2 C_{55}(z)U''''(z) + ik\left(1-0.25k^2l_y^2\right)\right.$$
$$C_{55}'(z)W(z) + ik(C_{13}(z)+C_{55}(z))W'(z) - 0.25ik^3l_y^2 C_{55}(z)W'(z) + 0.25ikl_y^2 C_{55}''(z)$$
$$\left.W'(z) + 0.5ikl_y^2 C_{55}'(z)W''(z) + 0.25ikl_y^2 C_{55}(z)W'''(z)\right)\pi(z) + \left(\left(1+0.25k^2l_y^2\right)C_{55}(z)\right.$$
$$\left.U'(z) - 0.5l_y^2\left(C_{55}(z)U''(z)\right)' + ik\left(1-0.25k^2l_y^2\right)C_{55}(z)W(z) + 0.5ikl_y^2\left(C_{55}(z)W'(z)\right)'\right)$$
$$\pi'(z) + \left(-0.25l_y^2 C_{55}(z)U''(z) + 0.25ikl_y^2 C_{55}(z)W'(z)\right)\pi''(z) = -\rho(z)\omega^2 U(z)$$

$$\tag{7a}$$

$$\left(-k^2\left(1+0.25k^2l_y^2\right)C_{55}(z)W(z) + \left(C_{33}(z)W'(z)\right)' + 0.25k^2l_y^2\left(C_{55}(z)W'(z)\right)' + ik\right.$$
$$(C_{13}(z)U(z))' + ik\left(1-0.25k^2l_y^2\right)C_{55}(z)U'(z) + 0.25ikl_y^2\left(C_{55}(z)U''(z)\right)'\right)\pi(z) +$$
$$\left(ikC_{13}(z)U(z) + 0.25ikl_y^2 C_{55}(z)U''(z) + C_{33}(z)W'(z) + 0.25k^2l_y^2 C_{55}(z)W'(z)\right)\pi'(z) = -\rho(z)\omega^2 W(z) \tag{7b}$$

$$\left(-k^2\left(1+0.25k^2l_z^2\right)C_{66}(z)V(z) + \left(C_{44}(z)V'(z)\right)' + 0.5k^2l_z^2 C_{44}'(z)V'(z) - 0.25k^2l_z^2\right.$$
$$C_{66}''(z)V(z) + 0.25k^2l_x^2 C_{44}(z)V''(z) + 0.25k^2l_z^2 C_{66}(z)V''(z) - 0.25l_x^2 C_{44}''(z)V''(z) - 0.5l_x^2 C_{44}'(z)V'''(z) - 0.25l_x^2 C_{44}(z)V''''(z)\right)\pi(z) + \left(C_{44}(z)V'(z)\left(1+0.5k^2l_x^2\right)\right.$$
$$-0.5k^2l_z^2 C_{66}'(z)V(z) - 0.5l_x^2\left(C_{44}(z)V''(z)\right)'\right)\pi'(z) - \left(0.25k^2l_z^2 C_{66}(z)V(z)\right.$$
$$\left.+0.25l_x^2 C_{44}(z)V''(z)\right)\pi''(z) = -\rho(z)\omega^2 V(z)$$
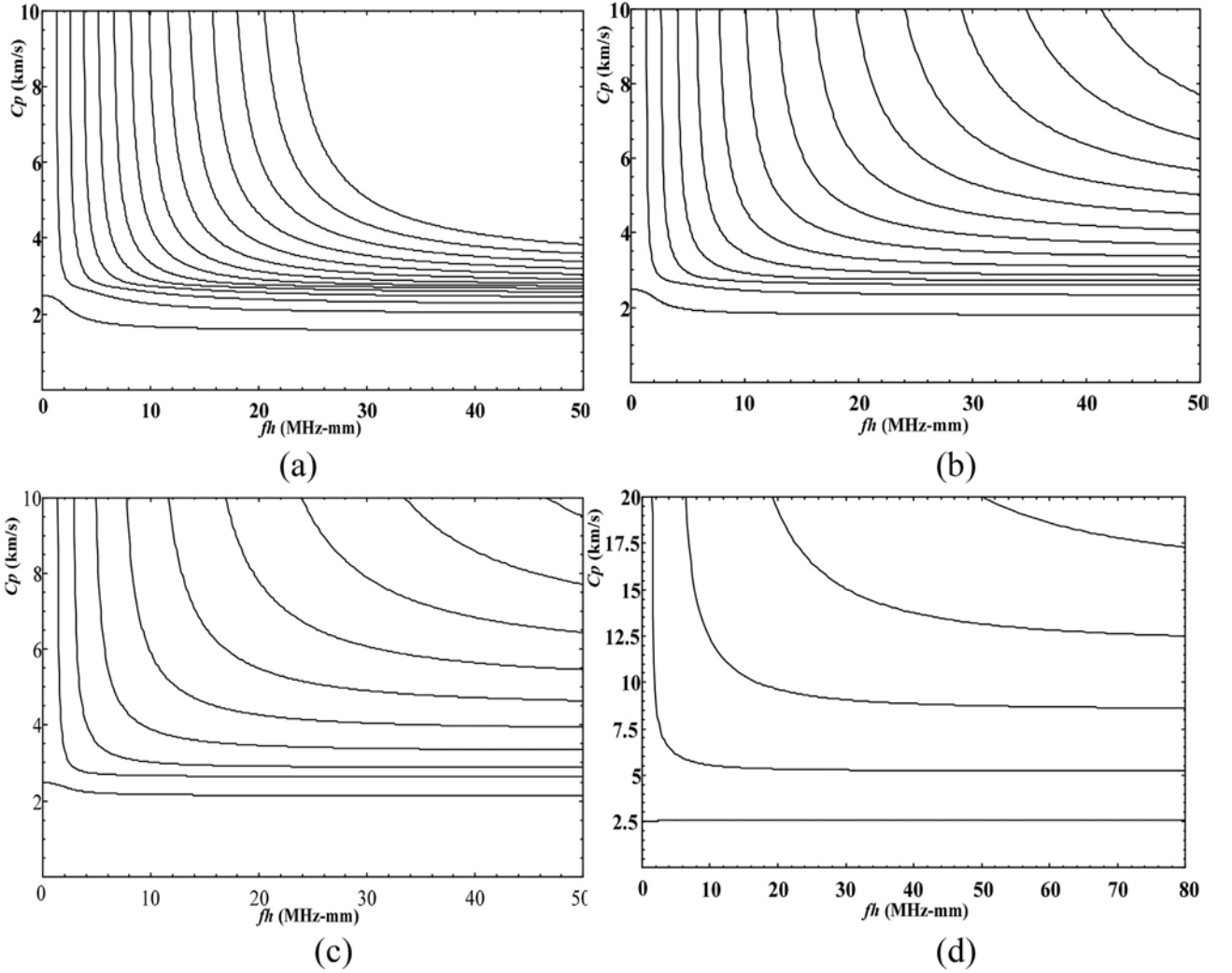
$$\tag{7c}$$

Fig. 7. Dispersion curves of SH waves in an FG plate made of BaTio$_3$ and human tibia with considering the effect of couple stress. (a): $L_x = 0.05$ (b): $L_x = 0.1$(c): $L_x = 0.2$ (d): $L_x = 1$.

Eq. (11) can be transformed into an eigenvalue problem. The eigenvalue is ω^2, and the eigenvector p_m^1, p_m^2, p_m^3 will give the wave displacement distributions. For Eqs. (11) and (3) $(M + 1)$ eigenvalues will be returned. As M increases, the numerically converged eigenvalues are the solutions of the wave dispersion modes.

3. Numerical result and discussion

3.1. Convergence analysis

The convergence of LOPM depends on the cut-off order value M. Before performing the method verifications, the value of M must be determined. The necessary error analysis is presented in Table 1. The FG plate made of human tibia and BaTiO$_3$ is consider. It can be seen from Table 1 that for a larger product of wavenumber and thickness kh, a larger value of M is required to ensure the convergence of LOPM.

In the present paper, if the relative error:

$$\Delta = (\text{Result } (M + 1) - \text{Result}(M))/\text{Result}(M) \leq 10^{-4} \tag{12}$$

It can be considered that the LOPM has reached convergence. Accordingly, the present method converges in the range of $kh = 0$–60 when $M = 12$. Theoretically, the larger the value of M, the closer the results are to the exact solution, but this will also increase the dimensions of the matrix, thus reducing the computational speed. In the subsequent examples, the adopted M value ensures the convergence of LOPM.

3.2. Method verifications

In the following calculation, the parameters l_i (for $i = x, y, z$) which characterize the material couple stress effect are taken in their normalized form as $L_i = l_i/h$. At present, rare references about guide waves in FG anisotropic couple-stressed plates are available. To validate the LOPM, a homogeneous aluminum nitride couple-stressed plate is solved and compared with the results from Ref. [8]. The longitudinal and transverse wave velocities used are $C_L = 11{,}225$ m/s and $C_T = 6220$ m/s, respectively. A good agreement between our results and those of Ref. [8] is reached, as shown in Fig. 1.

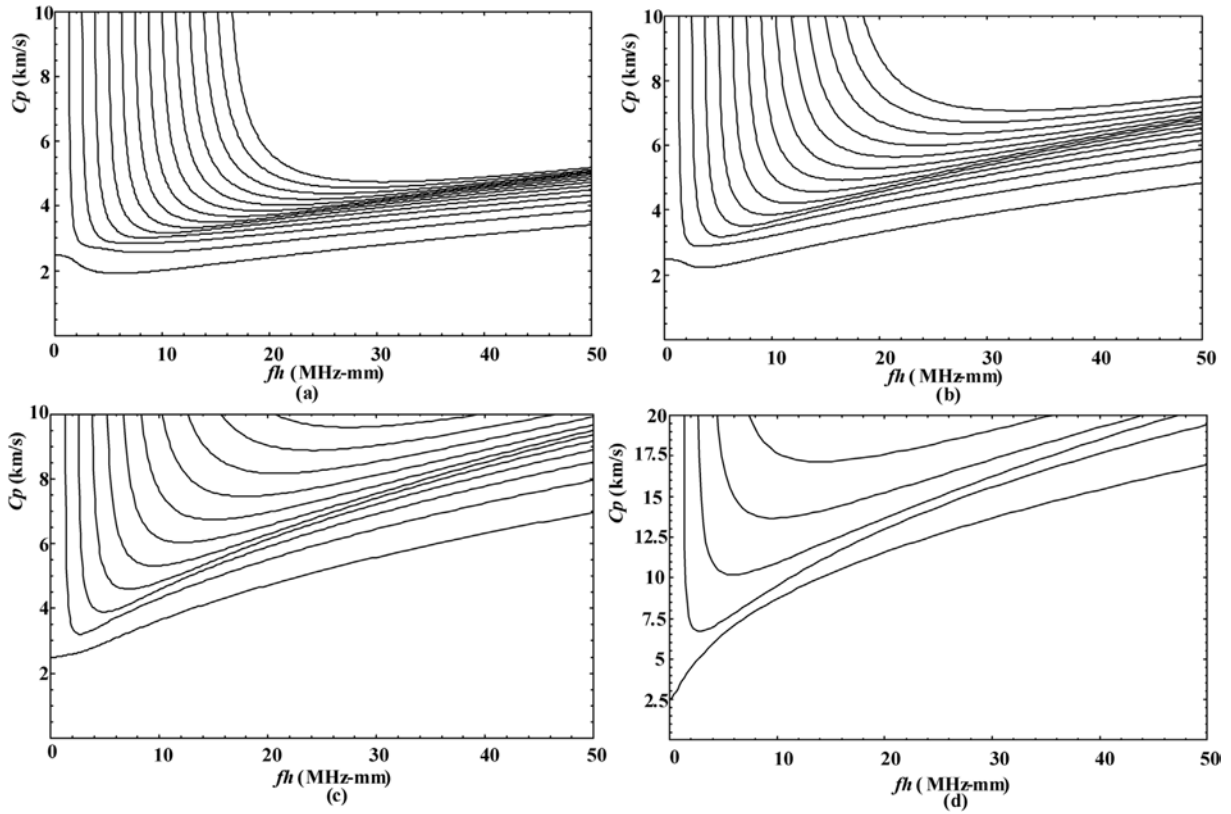Then, the solutions of an FG anisotropic plate are deduced by both the

Fig. 8. Dispersion curves of SH waves in an FG plate made of BaTio₃and human tibia with considering the effect of couple stress. (a): $L_z = 0.05$ (b): $L_z = 0.1$ (c): $L_z = 0.2$ (d): $L_z = 1$.

LOPM and GMM to verify the correctness of LOPM. The GMM solving process is attached at Appendix. The FG plate is composed of transversely isotropic materials PZT-4 and PZT-5A, in which their piezoelectric properties are ignored. The FG plate has a linearly gradient function $n = 1$. The material constants are listed in Table 2. The GMM method divides the FG plate into 25-layer multi-layer models. A good agreement between LOPM and GMM is reached, as shown in Fig. 2.

3.3. Lamb waves

In the case of an anisotropic material, firstly, Lamb waves are taken into consideration. The FG plate is made of two materials. The surfaces of $z = 0$ and $z = h$ are human tibia and BaTiO₃, respectively. The material constants are listed in Table 3 [37].

The influence of length scale parameters on the wave propagation behaviors is the focus of this section. Fig. 3 shows the Lamb wave dispersion curves for a homogeneous plate and for an FG plate by setting $L_y = 0$, equivalent to the classical theory of elasticity. The homogeneous plate is made by mixing two materials uniformly with the same volume fraction. The FG plate is mixed according to the law of power function with $n = 1$. The volume fractions of the materials in the two plates are equal. It can be observed that as the frequency increases, the Lamb wave modes for the homogeneous plates converge together rapidly, while the modes for the FG plates converge relatively slowly. Fig. 4 shows the Lamb wave dispersion curves with the values of L_y taken as: 0.1, 0.2, 0.4, and 0.8, respectively. It can be seen from the dispersion curves that for the FG plate without the couple stress, the wave velocity is usually a decreasing

function that changes with the frequency (except for the first mode), and converges to the Rayleigh-type surface mode as the frequency increases to the infinite. For the couple-stressed plate, a rising stage on the dispersion curves appears from low frequency and the phase velocities converge to higher surface ones. **The rising stage is even significant when the couple stress parameter L_y becomes large. The couple stress introduces a rotational gradient tensor, and the FG plate shows higher stiffness** [38]**.** This can explain that the couple stress effect increases the Lamb wave velocity and strengthens their dispersion degree.

From Fig. 4, a second effect on the dispersion curves by the couple stress for the FG plate is their wrinkle behavior. The larger the L_y is, the lower the frequency is at which the wrinkle appears, the higher the wrinkle amplitude becomes, and the occurrence range of the wrinkle phenomenon involves the higher-order lamb wave mode to the lower-order lamb wave mode. The wrinkle on the dispersion curves is manifested by the exchange of the phase velocity branches between two neighboring modes, and such exchange and separation are reproduced successively as the frequency increases or decreases. This phenomenon often exists for Lamb-type modes in the cases of material anisotropy, viscosity, material discontinuity (multilayer), wave leaky or absorption. It does the case here owing to the couple stress effect.

In order to illustrate the effect of material gradient characteristics on the Lamb waves in micro/nano-plates, Fig. 5 shows the Lamb wave dispersion curves in a homogeneous micro/nano-plate. It can be seen that the gradient characteristics make the Lamb wave phase velocity changing relatively gentle. Therefore, the amplitude of wrinkle in FG micro/nano-
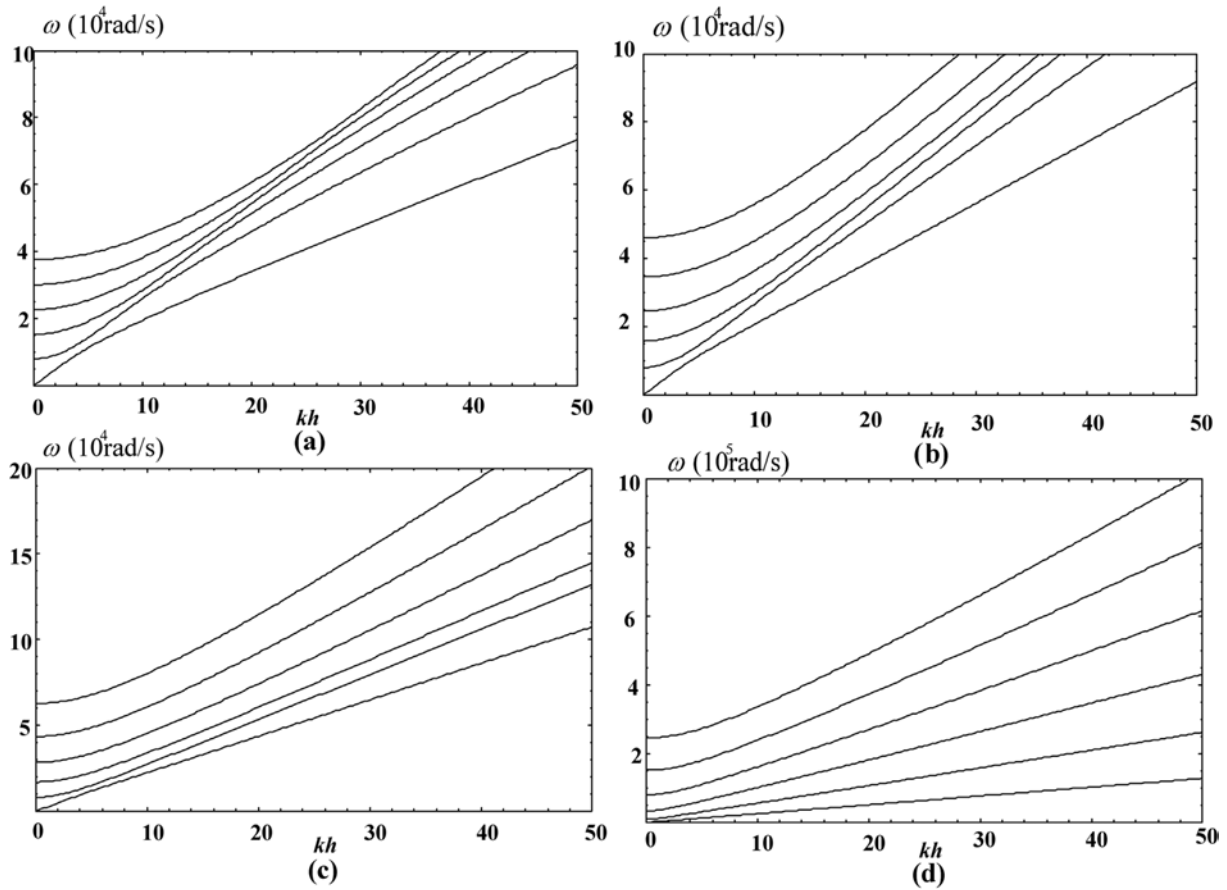
Fig. 9. Dispersion relationship between angular frequency ω and kh of SH wave in an FG plate. (a): Classical elasticity theory (b): $L_x = 0.1$ (c): $L_x = 0.2$ (d): $L_x = 1$.

plates is smaller than that of homogeneous micro/nano-plates, and the wrinkled range involved becomes larger.

3.4. SH wave

Fig. 6 shows the dispersion curves of SH waves in the FG plate obtained by using the classical theory of elasticity. Figs. 7 and 8 are the cases by using the couple stress theory. L_x and L_z are taken as: 0.05, 0.1, 0.2 and 1, respectively.

By comparing Figs. 6–8, it can be noticed that increasing the dimensionless length L_x and L_z can strengthen the degree of SH wave dispersion and increase the wave velocity in FG plates. The L_x does not change the overall trend of the dispersion curve, while L_z makes the dispersion curve of the SH wave show an upward trend. The larger the value of L_z, the faster the rise rate.

Figs. 9 and 10 show the dispersion relationship between the angular frequencies ω and kh. For easy observation, only the first few modes are given. It can be seen that the dimensionless length L_x increases the cut-off frequency of the SH wave, while L_z does not change the cut-off frequency.

4. Conclusions

The propagating characteristics of Lamb and SH waves in FG anisotropic micro/nano-plates are studied by using the extended LOPM. Different from the traditional matrix method, the polynomial method expands the displacement components into Legendre orthogonal polynomial series and automatically incorporates the boundary conditions. It does not need to solve the FG micro-structure hierarchically, nor does it need to solve the Christoffel equations to determine the wave propagation vectors in the anisotropic micro/nano-structure. It provides a more realistic analysis model for FG micro/nano-plates and has high computational efficiency. The main conclusions can be drawn based on the above numerical results:

(1) The Lamb wave dispersion curves of couple-stressed plates have a significant rising stage before convergence. The couple stress effect strengthens the degree of Lamb and SH wave dispersion, and improves the wave velocity.
(2) The couple stress effect causes wrinkles in the Lamb wave dispersion curves. As the length scale parameter increases, the wrinkling degree becomes stronger, and the wrinkled area move toward lower frequencies and higher phase velocities.
(3) The material gradient characteristics weaken the amplitude of wrinkles and widen the range of wrinkles in the Lamb wave dispersion curves.
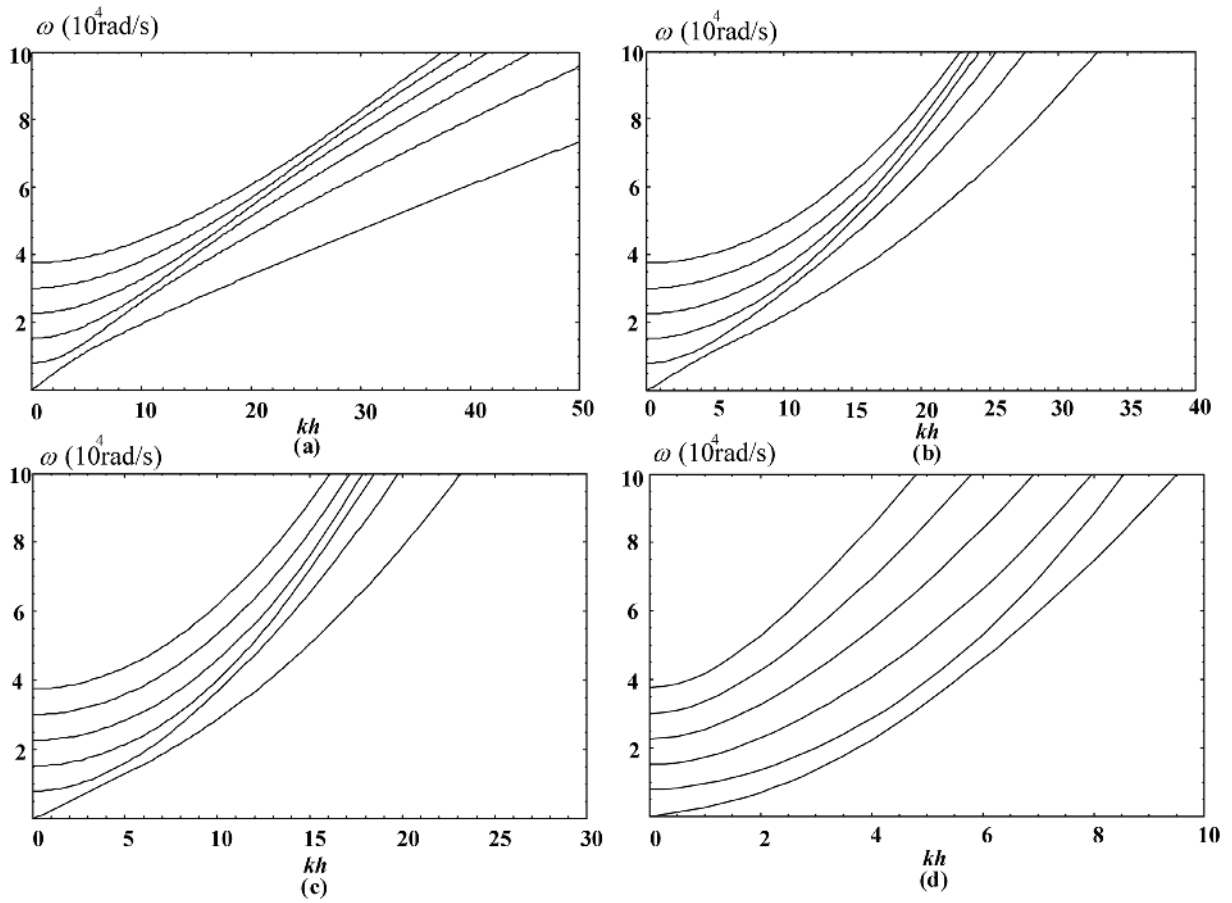
Fig. 10. Dispersion relationship between angular frequency ω and kh of SH wave in FG plate. (a): Classical elasticity theory (b): $L_z = 0.1$ (c): $L_z = 0.2$ (d): $L_z = 1$.

(4) The length scale parameter L_x increases the cut-off frequency but does not change the overall trend of the dispersion curve; L_z does not change the cut-off frequency but causes the dispersion curve to show an upward trend.

Author statement

Cancan Liu: Conceptualization, Formal analysis, Methodology, Validation, Writing - original draft. Jiangong Yu: Data curation, Supervision, Resources, Writing - review & editing. Weijiang Xu: Investigation, Methodology, Writing - review & editing. Xiaoming Zhang: Validation, Resources, Writing - review & editing. Xianhui Wang: Validation, Writing - review & editing. All authors read and contributed to the manuscript.

Declaration of competing interest

☒ The authors declare that they have no known competing financial interests or personal relationships that could have appeared to influence the work reported in this paper.

Appendix

The harmonic solutions of the mechanical displacements can be written as:

$$\left\{u_x^{(i)}, u_z^{(i)}\right\} = \left\{A^{(i)}, B^{(i)}\right\}\exp(ik(x + Q^{(i)}z) - i\omega t)i = 1, 2...N \tag{A1}$$

where the superscript (i) represents the i-th layer; $A^{(i)}$ and $B^{(i)}$ are the amplitude vectors of the mechanical displacements; and k and $kQ(i)$ are the wave vectors in x- and z-directions, respectively. Substituting Eq. (A1) into governing equations, the linear algebraic equations can be obtained as:

$$
\begin{bmatrix}
-C_{11}^{(i)}\ k^2 - C_{55}^{(i)}k^2\left(Q^{(i)}\right)^2 \\
-0.25\ C_{55}^{(i)}\ k^4 l_y^2\left(Q^{(i)}\right)^2 \\
-0.25\ C_{55}^{(i)}k^2 l_y^2\left(Q^{(i)}\right)^2 + \omega^2\rho^{(i)} \quad -C_{13}^{(i)}\ k^2 Q^{(i)} - C_{55}^{(i)}\ k^2 Q^{(i)} + \\
\qquad 0.25\ C_{55}^{(i)}\ k^4 l_y^2 Q^{(i)} + 0.25\ C_{55}^{(i)}\ k^4 l_y^2\left(Q^{(i)}\right)^3 - C_{33}^{(i)}\ k^2\left(Q^{(i)}\right)^2 - 0.25\ C_{55}^{(i)}\ k^4 l_y^2\left(Q^{(i)}\right)^2 + \omega^2\rho^{(i)} \\
-C_{13}^{(i)}\ k^2 Q^{(i)} - C_{55}^{(i)}\ k^2 Q^{(i)} + \\
0.25 C_{55}^{(i)}\ k^2 l_y^2 Q^{(i)} \qquad\qquad -C_{55}^{(i)}k^2 - 0.25 C_{55}^{(i)}\ k^4 l_y^2 \\
+0.25 C_{55}^{(i)}\ k^4 l_y^2\left(Q^{(i)}\right)^3
\end{bmatrix}
\begin{bmatrix} A^{(i)} \\ B^{(i)} \end{bmatrix} = 0 \tag{A2}
$$

In order to have nontrivial solutions of Eq. (A2), the determinant of the coefficient matrix must be equal to zero. There are six roots of $Q^{(i)}$ can be obtained, and the mechanical displacements can be reconstructed as linear combinations:

$$
u_x^{(i)} = \sum_{j=1}^{6} A_j^{(i)} \exp\left(ik\left(x + Q_j^{(i)}z\right) - i\omega t\right) \tag{A3}
$$

$$
u_z^{(i)} = \sum_{j=1}^{6} f_j^{(i)} A_j^{(i)} \exp\left(ik\left(x + Q_j^{(i)}z\right) - i\omega t\right) \tag{A4}
$$

$$
f_j^{(i)} = \frac{C_{11}^{(i)}k^2 + C_{55}^{(i)}k^2\left(Q_j^{(i)}\right)^2 + 0.25\ C_{55}^{(i)}k^4 l_y^2\left(Q_j^{(i)}\right)^2 + 0.25 C_{55}^{(i)}k^4 l_y^2\left(Q_j^{(i)}\right)^4 - \omega^2\rho^{(i)}}{-C_{13}^{(i)}k^2 Q_j^{(i)} - C_{55}^{(i)}k^2 Q_j^{(i)} + 0.25\ C_{55}^{(i)}k^4 l_y^2 Q_j^{(i)} + 0.25\ C_{55}^{(i)}k^4 l_y^2\left(Q_j^{(i)}\right)^3}
$$

Substituting Eq. (A3) and (A4) into constitutive relations, the stress, couple stress, rotation can be also reconstructed as linear combinations:

$$
\sigma_{zz}^{(i)} = \sum_{j=1}^{6} A_j^{(i)} \left(ikC_{13}^{(i)} + ikf_j^{(i)} C_{33}^{(i)} Q_j^{(i)}\right)\exp\left(ik\left(x + Q_j^{(i)}z\right) - i\omega t\right) \tag{A5}
$$

$$
\sigma_{zx}^{(i)} = \sum_{j=1}^{6} A_j^{(i)} C_{55}^{(i)}\left(ik - 0.25ik^3 l_y^2 - 0.25ik^3 l_y^2\left(Q_j^{(i)}\right)^2\right)f_j^{(i)}\exp\left(ik\left(x + Q_j^{(i)}z\right) - i\omega t\right)
$$
$$
+ \sum_{j=1}^{6} A_j^{(i)} C_{55}^{(i)}\left(\left(ik + 0.25\ ik^3 l_y^2\right)Q_j^{(i)} + 0.25\ ik^3 l_y^2\left(Q_j^{(i)}\right)^3\right)\exp\left(ik\left(x + Q_j^{(i)}z\right) - i\omega t\right) \tag{A6}
$$

$$
\mu_{zy}^{(i)} = \frac{1}{2}\sum_{j=1}^{6} A_j^{(i)} C_{55}^{(i)} l_y^2\left(k^2 f_j^{(i)} Q_j^{(i)} - k^2\left(Q_j^{(i)}\right)^2\right)\exp\left(ik\left(x + Q_j^{(i)}z\right) - i\omega t\right) \tag{A7}
$$

$$
\omega_y^{(i)} = \frac{1}{2}ik\sum_{j=1}^{6} A_j^{(i)}\left(-f_j^{(i)} + Q_j^{(i)}\right)\exp\left(ik\left(x + Q_j^{(i)}z\right) - i\omega t\right) \tag{A8}
$$

The boundary conditions can be expressed as:
At $z = 0$:

$$
\sigma_{zz}^1 = 0, \sigma_{zx}^1 = 0, \mu_{zy}^1 = 0. \tag{A9}
$$

At $z = h$:

$$
\sigma_{zz}^N = 0, \sigma_{zx}^N = 0, \mu_{zy}^N = 0. \tag{A10}
$$

At $z = h_i$, for $i = 1, 2 \dots N\text{-}1$:

$$
u_x^{i+1} = u_x^i, u_z^{i+1} = u_z^i, \sigma_{zx}^{i+1} = \sigma_{zx}^i, \sigma_{zz}^{i+1} = \sigma_{zz}^i, \mu_{zy}^{i+1} = \mu_{zy}^i, \omega_y^{i+1} = \omega_y^i. \tag{A11}
$$

Substitution of Eqs. (A3-A8) into Eqs. (A9-A11) yields the following linear equations:

$$
[B]\left\{A_j^{(i)}\right\} T = 0 \left(i = 1,\ 2\dots N,\ j = 1, 2\dots 6\right) \tag{A12}
$$

where [B] is a 6 N × 6 N matrix whose elements contain h, ω, k and material parameters. Then the dispersion relation can be obtained by solving $|B| = 0$ numerically.

References

[1] R.D. Mindlin, H.F. Tiersten, Effects of couple-stresses in linear elasticity, Arch. Ration. Mech. Anal. 11 (1) (1962) 415–448.

[2] F. Yang, A.C.M. Chong, D.C.C. Lam, P. Tong, Couple stress based strain gradient theory for elasticity, Int. J. Solid Struct. 39 (10) (2002) 2731–2743.

[3] W. Chen, X. Li, A new modified couple stress theory for anisotropic elasticity and microscale laminated Kirchhoff plate model, Arch. Appl. Mech. 84 (2014) 323–341.

[4] Wanli Yang, Dan He, Bending, free vibration and buckling analyses of anisotropic layered micro-plates based on a new size-dependent model, Compos. Struct. 189 (2018) 137–147.

[5] F. Mehralian, Y.T. Beni, R. Ansari, On the size dependent buckling of anisotropic piezoelectric cylindrical shells under combined axial compression and lateral pressure, Int. J. Mech. Sci. 119 (2016) 155–169.

[6] K.B. Mustapha, Z.W. Zhong, Wave propagation characteristics of a twisted micro scale beam, Int. J. Eng. Sci. 53 (2012) 46–57.

[7] V. Sharma, S. Kumar, Velocity dispersion in an elastic plate with microstructure: effects of characteristic length in a couple stress model, Meccanica 49 (5) (2014) 1083–1090.

[8] B. Ghodrati, A. Yaghootian, A. Ghanbar Zadeh, et al., Lamb wave extraction of dispersion curves in micro/nano-plates using couple stress theories, Waves Random Complex Media (2017) 1–20.

[9] Niels Saabye Ottosen, Christer Ljung MattiRistinmaa, Rayleigh waves obtained by the indeterminate couple-stress theory, Eur. J. Mech. Solid. 19 (6) (2000) 929–947.

[10] Y.Z. Wang, F.M. Li, K. Kishimoto, Scale effects on the longitudinal wave propagation in nanoplates, Physica E Low-dimensional Systems and Nanostructures 42 (5) (2010) 1356–1360.

[11] J. Chen, J. Guo, E. Pan, Wave propagation in magneto-electro-elastic multilayered plates with nonlocal effect, J. Sound Vib. 400 (2017) 550–563.

[12] F. Zhu, E. Pan, Z. Qian, Y. Wang, Dispersion curves, mode shapes, stresses and energies of SH and Lamb waves in layered elastic nanoplates with surface/interface effect, Int. J. Eng. Sci. 142 (2019) 170–184.

[13] S. Narendar, S. Gopalakrishnan, Study of terahertz wave propagation properties in nanoplates with surface and small-scale effects, Int. J. Mech. Sci. 64 (1) (2012) 221–231.

[14] H. Zeighampour, Y.T. Beni, M.B. Dehkordi, Wave propagation in viscoelastic thin cylindrical nanoshell resting on a visco-Pasternak foundation based on nonlocal strain gradient theory, Thin-Walled Struct. 122 (2018) 378–386.

[15] J.N. Sharma, S. Kumar, Lamb waves in micropolar thermoelastic solid plates immersed in liquid with varying temperature, Meccanica 44 (3) (2009) 305–319.

[16] T. Fu, X. Wu, Z. Xiao, Z. Chen, Thermoacoustic response of porous FGM cylindrical shell surround by elastic foundation subjected to nonlinear thermal loading, Thin-Walled Struct. 156 (2020) 106996.

[17] T. Fu, X. Wu, Z. Xiao, Z. Chen, Study on dynamic instability characteristics of functionally graded material sandwich conical shells with arbitrary boundary conditions, Mech. Syst. Signal Process. 151 (2021) 107438.

[18] Arefi Mohammad, M.R. Bidgoli, T. Rabczuk, Thermo-mechanical buckling behavior of FG GNP reinforced micro plate based on MSGT, Thin-Walled Struct. 142 (2019) 444–459.

[19] S. Sahmani, B. Safaei, Nonlinear free vibrations of bi-directional functionally graded micro/nano-beams including nonlocal stress and microstructural strain gradient size effects, Thin-Walled Struct. 140 (2019) 342–356.

[20] L. Li, Y. Hu, L. Ling, Flexural wave propagation in small-scaled functionally graded beams via a nonlocal strain gradient theory, Compos. Struct. 133 (2015) 1079–1092.

[21] M. Arefi, A.M. Zenkour, Analysis of wave propagation in a functionally graded nanobeam resting on visco-Pasternak's foundation, Theoretical and Applied Mechanics Letters 7 (2017) 121–178.

[22] B. Karami, M. Janghorban, L. Li, On guided wave propagation in fully clamped porous functionally graded nanoplates, Acta Astronaut. 143 (2018) 380–390.

[23] Huu-Tai Thai, Dong-Ho Choi, Size-dependent functionally graded Kirchhoff and Mindlin plate models based on a modified couple stress theory, Compos. Struct. 95 (2013) 142–153.

[24] Y. Yuan, K. Zhao, Y. Han, S. Sahmani, B. Safaei, Nonlinear oscillations of composite conical microshells with in-plane heterogeneity based upon a couple stress-based shell model, Thin-Walled Struct. 154 (2020) 106857.

[25] P.R. Sajanlal, T.S. Sreeprasad, A.K. Samal, Anisotropic nanomaterials: structure, growth, assembly, and functions, Nano Rev. 2 (2011) 5883.

[26] Behrouz Karami, M. Janghorban, A. Tounsi, Variational approach for wave dispersion in anisotropic doubly-curved nanoshells based on a new nonlocal strain gradient higher order shell theory, Thin-Walled Struct. 129 (2018) 251–264.

[27] C. Liu, J. Yu, B. Zhang, X. Zhang, Reflection and transmission of elastic waves in the multilayered orthotropic couple-stressed plates sandwiched between two elastic half-spaces, Appl. Math. Model. 75 (2019) 52–72.

[28] J. Guo, J. Chen, E. Pan, Size-dependent behavior of functionally graded anisotropic composite plates, Int. J. Eng. Sci. 106 (2016) 110–124.

[29] X. Zhang, Z. Li, X. Wang, J. Yu, The fractional Kelvin-Voigt model for circumferential guided waves in a viscoelastic FGM hollow cylinder, Appl. Math. Model. 89 (2021) 299–313.

[30] X. Wang, F. Li, X. Zhang, H. Qiao, Thermoelastic guided wave in fractional order functionally graded plates: an analytical integration Legendre polynomial approach, Compos. Struct. (2020) 256.

[31] C. Othmani, F. Takali, A. Njeh, Ben Ghozlen, Hédi Mohamed, Numerical simulation of lamb waves propagation in a functionally graded piezoelectric plate composed of gaas-alas materials using legendre polynomial approach, Optik 142 (2017) 401–411.

[32] C. Liu, J. Yu, W. Xu, X. Zhang, B. Zhang, Theoretical study of elastic wave propagation through a functionally graded micro-structured plate base on the modified couple-stress theory, Meccanica 55 (2020) 1153–1167.

[33] H.S. Shen, Z.X. Wang, Assessment of Voigt and Mori–Tanaka models for vibration analysis of functionally graded plates, Compos. Struct. 94 (7) (2012) 2197–2208.

[34] J.E. Lefebvre, J.G. Yu, F.E. Ratolojanahary, L. Elmaimouni, W.J. Xu, T. Gryba, Mapped orthogonal functions method applied to acoustic waves-based devices, AIP Adv. 6 (2016), 065307, 6.

[35] J. Yu, J.E. Lefebvre, Y.Q. Guo, Free-ultrasonic waves in multilayered piezoelectric plates: an improvement of the Legendre polynomial approach for multilayered structures with very dissimilar materials, Compos. B Eng. 51 (2013) 260–269.

[36] G.M. Kulikov, S.V. Plotnikova, A new approach to three-dimensional exact solutions for functionally graded piezoelectric laminated plates, Compos. Struct. 106 (2013) 33–46.

[37] J. Guo, J. Chen, E. Pan, Free vibration of three-dimensional anisotropic layered composite nanoplates based on modified couple-stress theory, Physica E Low Dimensional Systems & Nanostructures 87 (2017) 98–106.

[38] Y.S. Li, E.S. Pan, Static bending and free vibration of a functionally graded piezoelectric microplate based on the modified couple-stress theory, Int. J. Eng. Sci. 97 (2015) 40–59.